# Astrofisica Nucleare e Subnucleare

## Design of Future High Energy Gamma-ray Telescopes

## Journal Club #1

# Title and Abstract

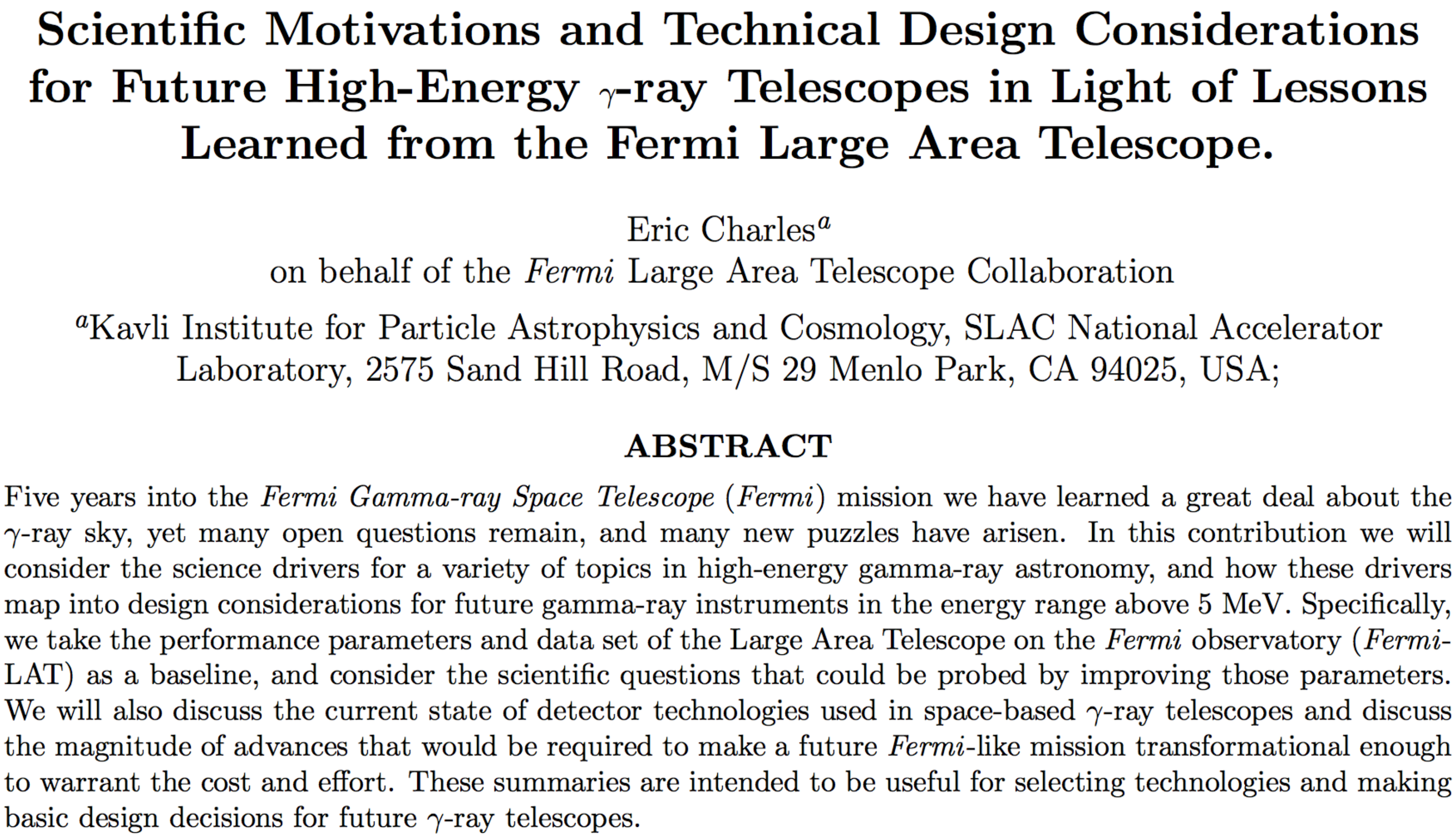

## Scientific Motivations and Technical Design Considerations for Future High-Energy $\gamma$-ray Telescopes in Light of Lessons Learned from the Fermi Large Area Telescope.

Eric Charles[a]
on behalf of the *Fermi* Large Area Telescope Collaboration

[a]Kavli Institute for Particle Astrophysics and Cosmology, SLAC National Accelerator Laboratory, 2575 Sand Hill Road, M/S 29 Menlo Park, CA 94025, USA;

### ABSTRACT

Five years into the *Fermi Gamma-ray Space Telescope* (*Fermi*) mission we have learned a great deal about the $\gamma$-ray sky, yet many open questions remain, and many new puzzles have arisen. In this contribution we will consider the science drivers for a variety of topics in high-energy gamma-ray astronomy, and how these drivers map into design considerations for future gamma-ray instruments in the energy range above 5 MeV. Specifically, we take the performance parameters and data set of the Large Area Telescope on the *Fermi* observatory (*Fermi*-LAT) as a baseline, and consider the scientific questions that could be probed by improving those parameters. We will also discuss the current state of detector technologies used in space-based $\gamma$-ray telescopes and discuss the magnitude of advances that would be required to make a future *Fermi*-like mission transformational enough to warrant the cost and effort. These summaries are intended to be useful for selecting technologies and making basic design decisions for future $\gamma$-ray telescopes.

# Introduction

- It is worth noting that these missions concepts feature a variety of detector technologies, include a Silicon tracker/ Tungsten converter similar to the LAT (GAMMA 400), a Silicon tracker without conversion layers (Gamma-Light, a Silicon PIN diode tracker (DAMPE), a low-density gaseous time projection chamber (TPC, AdEPT), a high-pressure gaseous TPC (HARPO), and a liquid Argon TPC (LArGO).

- This paper is organized as follows: in Sec. 2 we will discuss the performance of the Fermi-LAT, taking it as a reference for future high-energy γ-ray missions; in Sec. 3 we will survey topics in high-energy γ-ray astronomy, and discuss which aspects of the instrument performance are most important for each topic; then in Sec. 4 we will discuss detector design considerations and available technologies for future high-energy γ-ray missions; finally, we will discuss and summarize our findings in Sec. 5.

# The Large Area Telescope

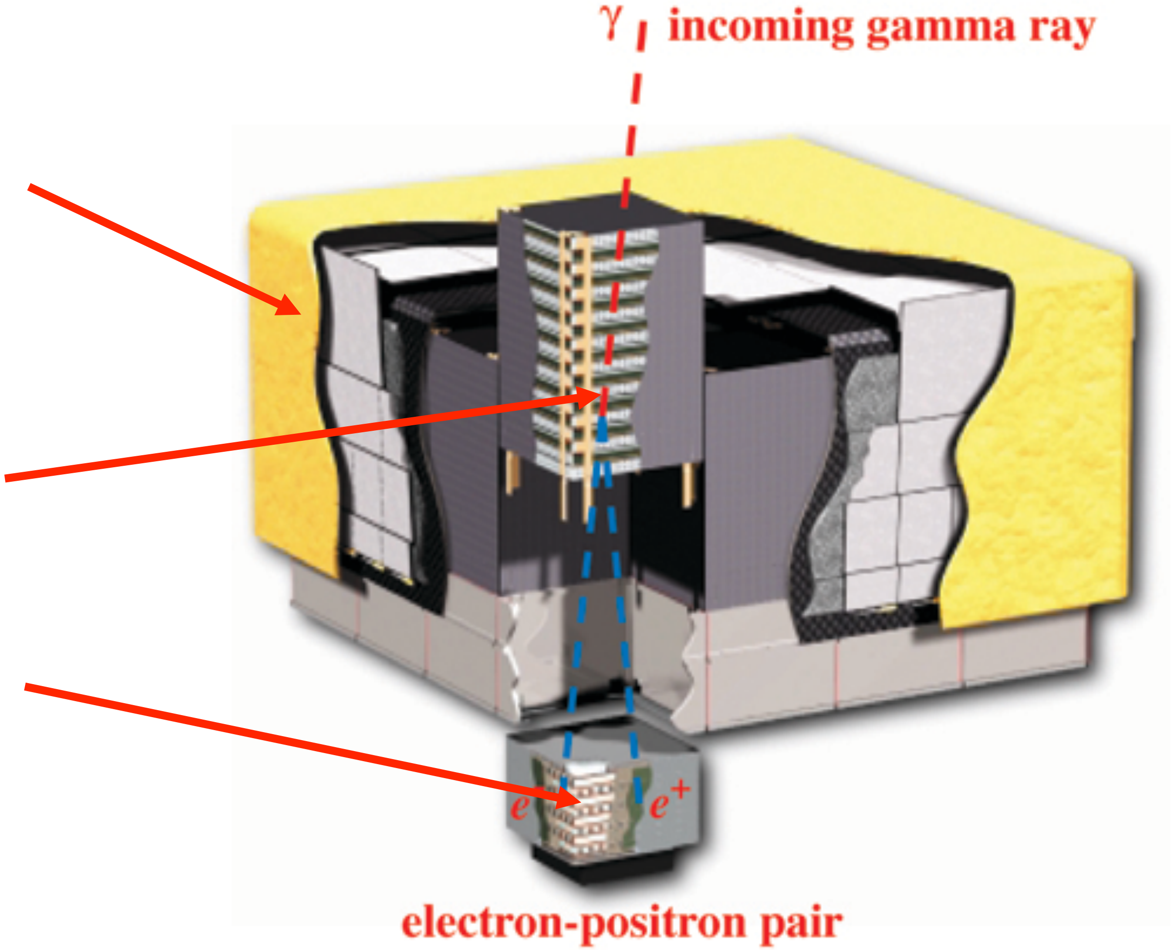

- Tiled Anticoincidence Detectors
- Silicon strip detectors interleaved with Tungsten converter
- Cesium Iodide hodoscopic calorimeter

# Performance of the LAT

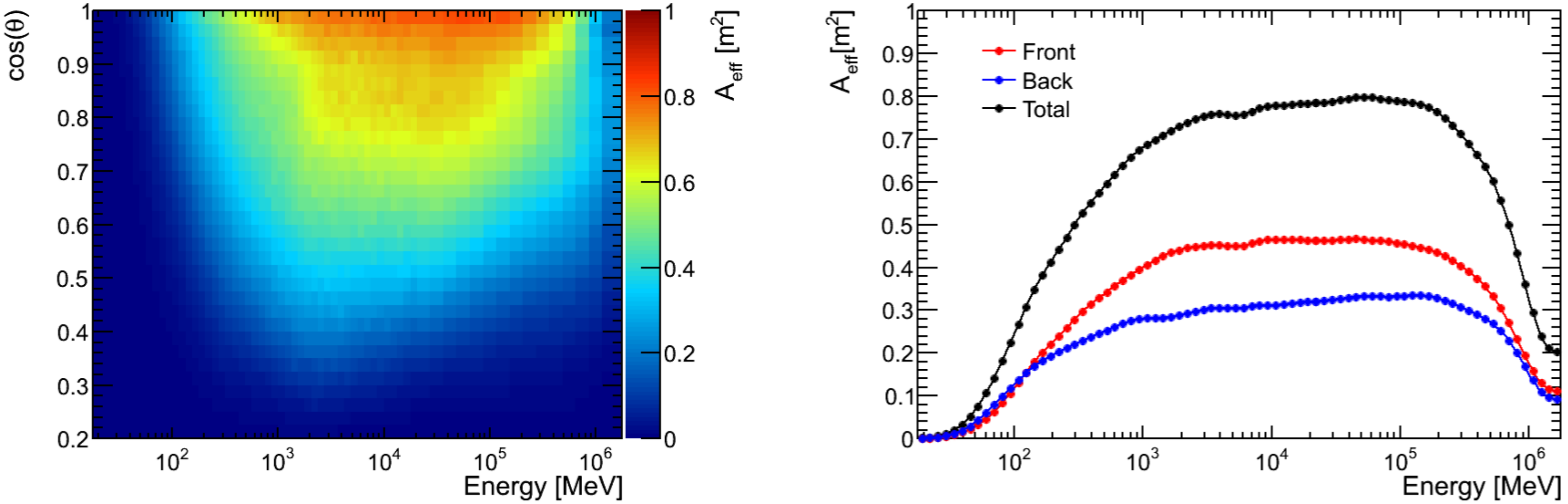

Figure 1. LAT $A_{\mathrm{eff}}$ in $m^2$ as a function of energy and off-axis angle ($\theta$) (left), and as a function of energy for on-axis events (right). Front and back refer to events that convert in different sections of the tracker, which result in large difference in spatial and energy resolution.

# Performance of the LAT

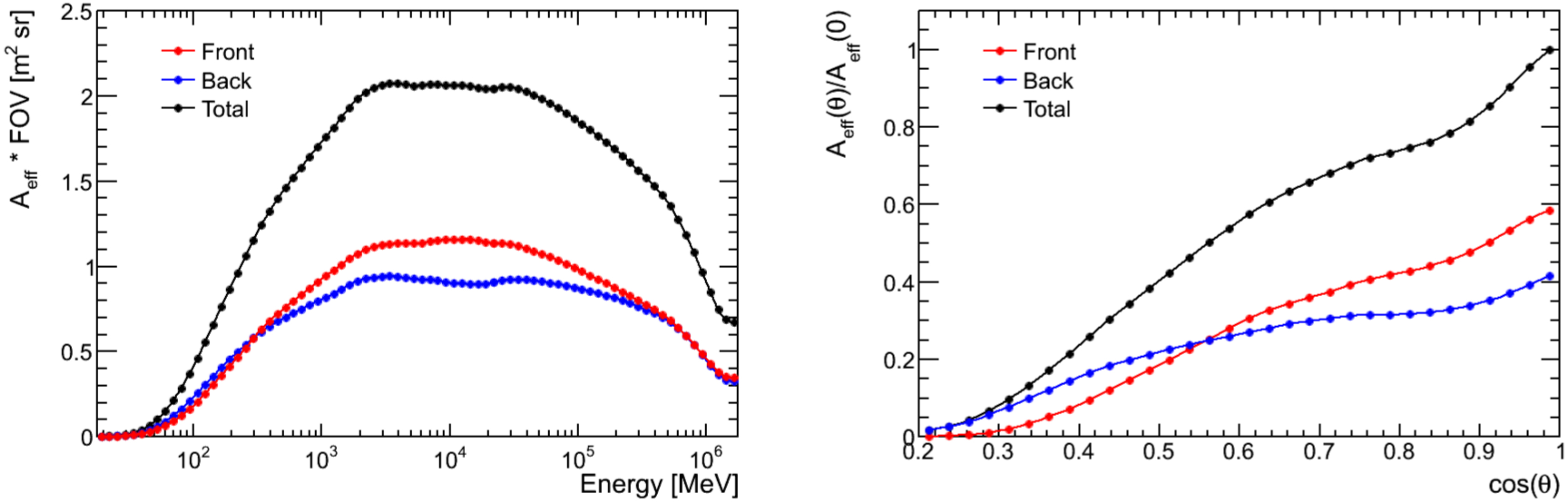

Figure 2. LAT Acceptance in m$^2$sr as a function of energy (left), and $\theta$-dependence of the $A_{\text{eff}}$ at 1 GeV (right).

# Performance of the LAT

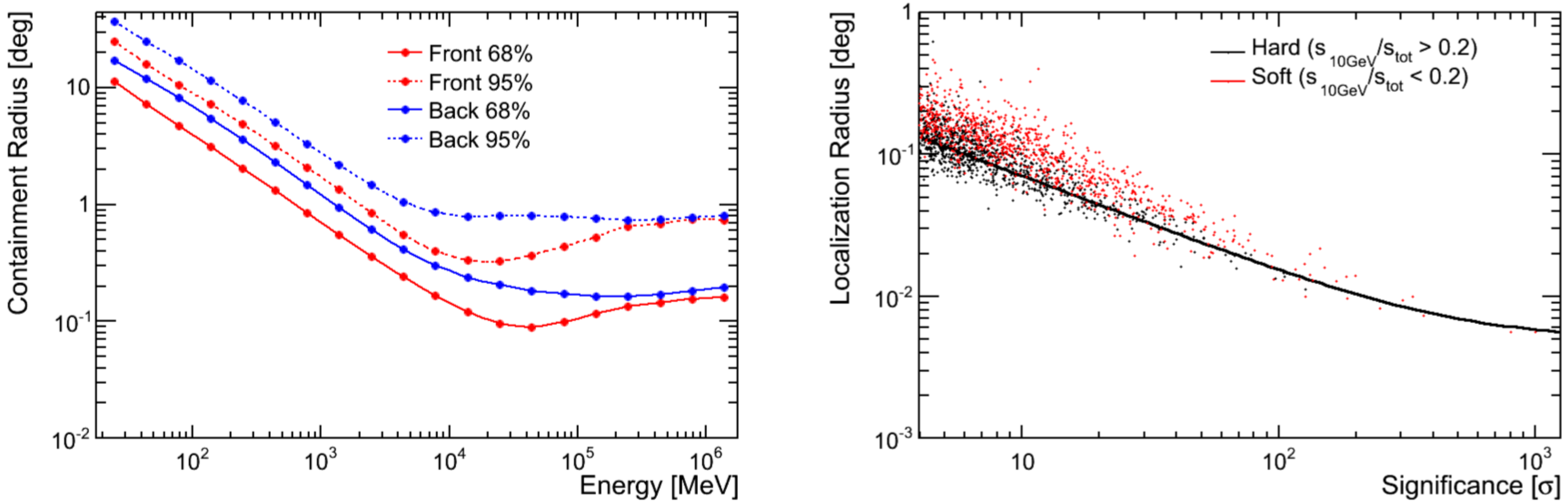

Figure 3. Containment radii of the acceptance-averaged PSF as a function of energy (left). LAT localization precision (given radius of the 95% error circle) as a function of source significance, values are taken from the 2FGL catalog (right). The solid line in the right plot shows a fit to the hard sources only, i.e., those sources for which the detection significance above 10 GeV is at least 20% of the total detection significance. The fit parameter values are given in the text.

# Performance of the LAT

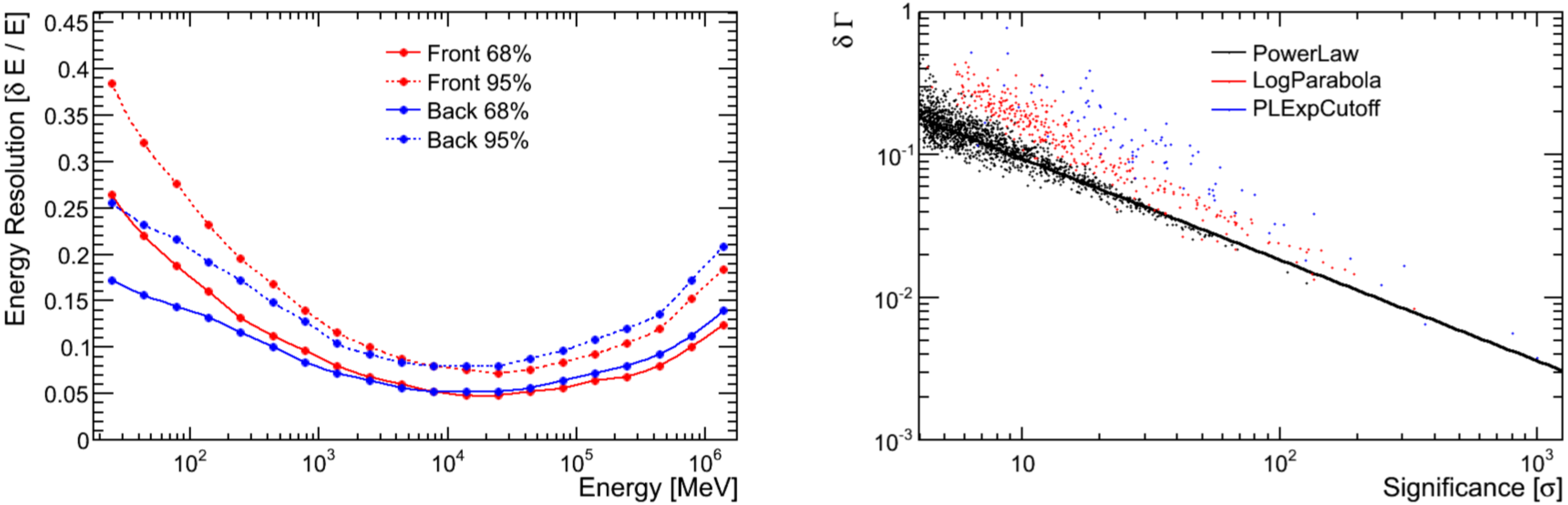

Figure 4. Acceptance-averaged energy resolution as a function of energy (left), and LAT spectral precision (i.e., the uncertainty on the power-law index) as a function of source significance; values are taken from 2FGL catalog (right). The solid line in the right plot shows a fit to the power-law sources only; the fit parameter values are given in the text. The additional free parameters in the other spectral forms result in larger statistical uncertainty in the spectral index.

# Performance of the LAT

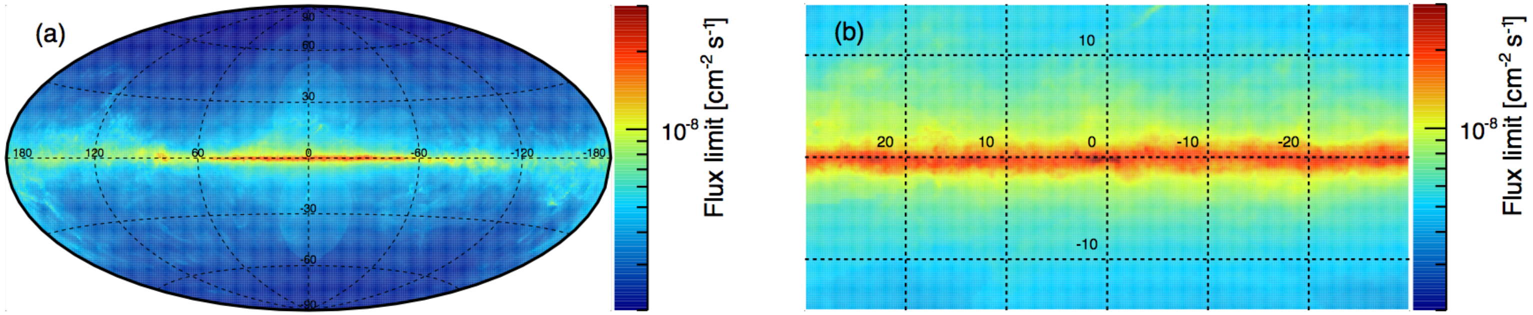

Figure 5. Flux above 100 MeV required for $5\sigma$ sensitivity for a point source with power-law spectrum with index $\Gamma = 2$. The calculation assumes a 4-year exposure. The entire sky (left) and a zoom on the Galactic center (right) are shown.

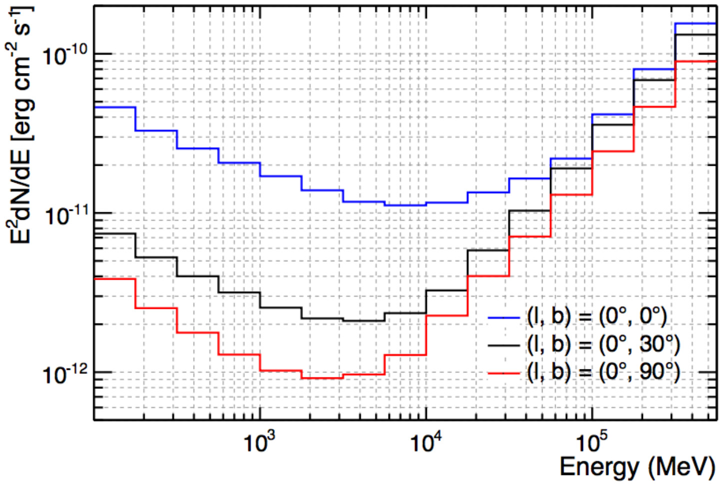

Figure 6. Differential sensitivity for a point source; the calculation assumes a 3-year exposure, 4 bins per energy decade. Requirements are $5\sigma$ sensitivity and at least 10 counts per bin. The sensitivity is shown at three locations in the sky: at the Galactic pole, at an intermediate latitude and on the Galactic plane.

# Performance of the LAT

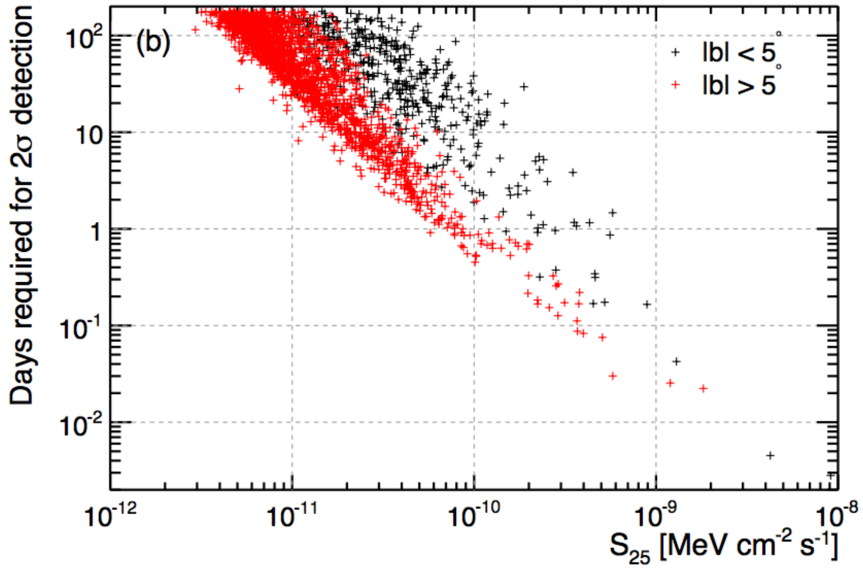

Figure 7. LAT sensitivity to variability of all 2FGL catalog sources, showing the estimated time required to reach a $2\sigma$ detection as a function of the integral energy flux between 100 MeV and 100 GeV ($S_{25}$) for both low- and high- Galactic latitude sources.

# Scientific Highlights of the LAT

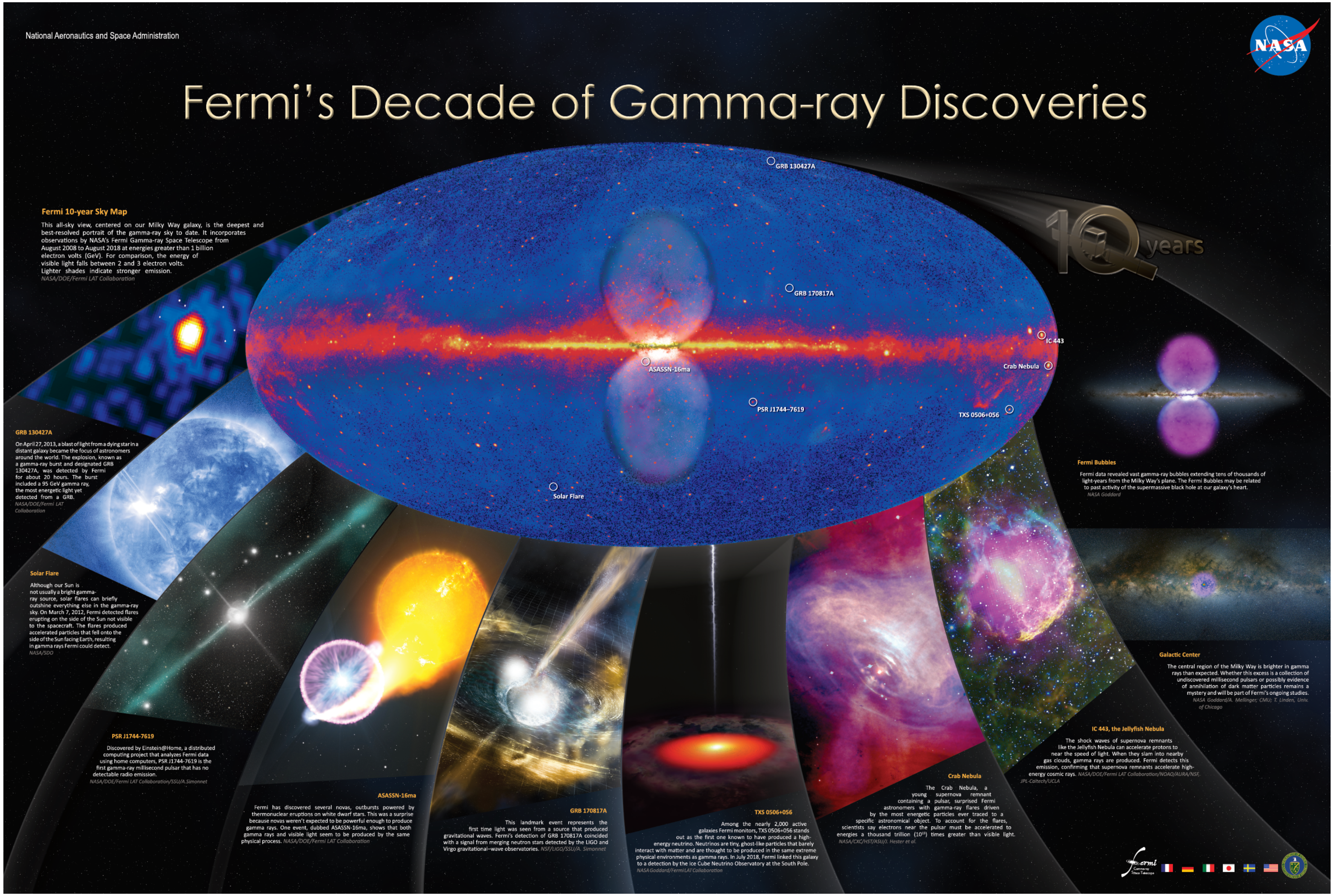

National Aeronautics and Space Administration

## Fermi's Decade of Gamma-ray Discoveries

**Fermi 10-year Sky Map**

This all-sky view, centered on our Milky Way galaxy, is the deepest and best-resolved portrait of the gamma-ray sky to date. It incorporates observations by NASA's Fermi Gamma-ray Space Telescope from August 2008 to August 2018 at energies greater than 1 billion electron volts (GeV). For comparison, the energy of visible light falls between 2 and 3 electron volts. Lighter shades indicate stronger emission. *NASA/DOE/Fermi LAT Collaboration*

**GRB 130427A**

On April 27, 2013, a blast of light from a dying star in a distant galaxy became the focus of astronomers around the world. The explosion, known as a gamma-ray burst and designated GRB 130427A, was detected by Fermi for about 20 hours. The burst included a 95 GeV gamma ray, the most energetic light yet detected from a GRB. *NASA/DOE/Fermi LAT Collaboration*

**Solar Flare**

Although our Sun is not usually a bright gamma-ray source, solar flares can briefly outshine everything else in the gamma-ray sky. On March 7, 2012, Fermi detected flares erupting on the side of the Sun not visible to the spacecraft. The flares produced accelerated particles that fell onto the side of the Sun facing Earth, resulting in gamma rays Fermi could detect. *NASA/SDO*

**PSR J1744-7619**

Discovered by Einstein@Home, a distributed computing project that analyzes Fermi data using home computers, PSR J1744-7619 is the first gamma-ray millisecond pulsar that has no detectable radio emission. *NASA/DOE/Fermi LAT Collaboration/SSU/A.Simonnet*

**ASASSN-16ma**

Fermi has discovered several novas, outbursts powered by thermonuclear eruptions on white dwarf stars. This was a surprise because novas weren't expected to be powerful enough to produce gamma rays. One event, dubbed ASASSN-16ma, shows that both gamma rays and visible light seem to be produced by the same physical process. *NASA/DOE/Fermi LAT Collaboration*

**GRB 170817A**

This landmark event represents the first time light was seen from a source that produced gravitational waves. Fermi's detection of GRB 170817A coincided with a signal from merging neutron stars detected by the LIGO and Virgo gravitational–wave observatories. *NSF/LIGO/SSU/A. Simonnet*

**TXS 0506+056**

Among the nearly 2,000 active galaxies Fermi monitors, TXS 0506+056 stands out as the first one known to have produced a high-energy neutrino. Neutrinos are tiny, ghost-like particles that barely interact with matter and are thought to be produced in the same extreme physical environments as gamma rays. In July 2018, Fermi linked this galaxy to a detection by the Ice Cube Neutrino Observatory at the South Pole. *NASA Goddard/Fermi LAT Collaboration*

**Crab Nebula**

The Crab Nebula, a young supernova remnant containing a pulsar, surprised Fermi astronomers with gamma-ray flares driven by the most energetic particles ever traced to a specific astronomical object. To account for the flares, scientists say electrons near the pulsar must be accelerated to energies a thousand trillion ($10^{15}$) times greater than visible light. *NASA/CXC/HST/ASU/J. Hester et al.*

**IC 443, the Jellyfish Nebula**

The shock waves of supernova remnants like the Jellyfish Nebula can accelerate protons to near the speed of light. When they slam into nearby gas clouds, gamma rays are produced. Fermi detects this emission, confirming that supernova remnants accelerate high-energy cosmic rays. *NASA/DOE/Fermi LAT Collaboration/NOAO/AURA/NSF, JPL-Caltech/UCLA*

**Galactic Center**

The central region of the Milky Way is brighter in gamma rays than expected. Whether this excess is a collection of undiscovered millisecond pulsars or possibly evidence of annihilation of dark matter particles remains a mystery and will be part of Fermi's ongoing studies. *NASA Goddard/A. Mellinger, CMU; T. Linden, Univ. of Chicago*

**Fermi Bubbles**

Fermi data revealed vast gamma-ray bubbles extending tens of thousands of light-years from the Milky Way's plane. The Fermi Bubbles may be related to past activity of the supermassive black hole at our galaxy's heart. *NASA Goddard*

Table 1. Summary of the importance of instrument performance parameters for science topics in high-energy $\gamma$-ray astronomy. Key performance parameter are marked as "1", other important parameters as "2", marginally relevant parameters as "3" and irrelevant parameters are unmarked. The performance parameters are background rejection ("Bkg"), point-source sensitivity ("Source"), on-axis $A_{\rm eff}$ ("$A_{\rm eff}$"), field-of-view (FOV), point-source localization ("PSF Loc."), extension detection/ associating a given $\gamma$ ray with a particular source ("PSF Ext."), energy bandpass ("Band"), energy resolution ("Energy Res."), spectral resolution ("Energy spec."), relative timing and deadtime between readouts ("Timing Rel.") and absolute timing ("Timing Abs.").

| | | | Acceptance | | PSF | | Energy | | | Timing | |
|---|---|---|---|---|---|---|---|---|---|---|---|
| Topic | Bkg. | Source | $A_{\rm eff}$ | FOV | Loc. | Ext. | Band | Res. | Spec. | Rel. | Abs. |
| GRB Detection | 2 | 1 | 1 | 1 | 3 | - | 2 | - | - | - | - |
| GRB Localization | 2 | 2 | 2 | 2 | 1 | - | - | - | - | - | - |
| GRB Modeling | 2 | 2 | 1 | 1 | - | 2 | 1 | 2 | 1 | 2 | 3 |
| GRB EBL Studies | 2 | 3 | 1 | 1 | - | 2 | 2 | 2 | - | - | 3 |
| GRB LIV Studies | 3 | - | 1 | 1 | - | 2 | 2 | 2 | - | 1 | 2 |
| AGN Pop. Studies | 3 | 1 | 1 | 2 | 1 | - | 1 | 3 | 2 | - | - |
| AGN Variability | 3 | 1 | 1 | 1 | - | - | 2 | 3 | 2 | - | - |
| AGN EBL Studies | 3 | 1 | 1 | 2 | - | 1 | 2 | 3 | 3 | - | - |
| Nearby Galaxies | 3 | 1 | 1 | 2 | 3 | 1 | 1 | 3 | 2 | - | - |
| Galactic Diffuse | 1 | 2 | 2 | 2 | - | 1 | 3 | 3 | 2 | - | - |
| Extra-Galactic Diffuse | 1 | 2 | 2 | 2 | - | 2 | 1 | 3 | 2 | - | - |
| Radio Timed Pulsars | 3 | 1 | 1 | 1 | - | 2 | 2 | 3 | 2 | 3 | 1 |
| Blind Search Pulsars | 2 | 2 | 1 | 1 | 1 | 2 | 2 | 3 | 2 | 3 | 1 |
| Pulsar Radio Targets | 3 | 1 | 1 | 2 | 1 | - | 3 | 3 | 3 | - | - |
| Pulsar Modeling | 3 | 2 | 1 | 2 | - | 2 | 2 | 2 | 1 | 3 | 1 |
| SNR / PWN | 2 | 2 | 1 | 2 | 3 | 1 | 1 | 2 | 1 | - | - |
| X-ray Binaries | 2 | 1 | 1 | 2 | 2 | 3 | 1 | 3 | 2 | - | - |
| Galactic Novae | 2 | 1 | 1 | 2 | 1 | 3 | 1 | 3 | 2 | - | - |
| Earth | - | - | 3 | 2 | - | 3 | 1 | 3 | 1 | - | - |
| Sun / Moon | 2 | 1 | 1 | 2 | 3 | 1 | 1 | 3 | 2 | - | - |
| Solar Flares | 2 | 1 | 1 | 1 | 1 | 3 | 1 | 3 | 2 | 2 | - |
| TGFs | - | - | 2 | 2 | - | - | 3 | - | - | 1 | 2 |
| DM dSph | 2 | 1 | 1 | 2 | - | 2 | 2 | 3 | 2 | - | - |
| DM Galaxy Clusters | 2 | 1 | 1 | 2 | - | 1 | 2 | 3 | 2 | - | - |
| DM Inner Galaxy | 3 | 2 | 2 | 2 | 1 | 1 | 1 | 3 | 1 | - | - |
| DM Lines | 1 | - | 2 | 2 | - | 3 | 1 | 1 | 1 | - | - |

# Design considerations

- Summary of interaction processes
  - Radiation Length
  - Pair conversion and Compton scatter
  - Energy Losses of Electrons and Positrons
  - Electromagnetic Shower Propagation
  - Multiple Coulomb Scattering
  - Plane thickness and Hit spacing

# Design considerations

- Power Budget and Heat Dissipation.
- Data Transmission.
- Consumables and Reliability.
- Mass and Size.

# Implication for Instrument Performance

- Background rejection versus FOV.
- Aeff versus PSF.
- Sky-survey versus Pointed Observations
- PSF, Timing Resolution versus Power Budget.
- Energy Resolution versus Aeff and FOV.
- Size versus Complexity of Event Readout, Triggering and Filtering.
- Optimal Orbit.

# Implication for Instrument Performance

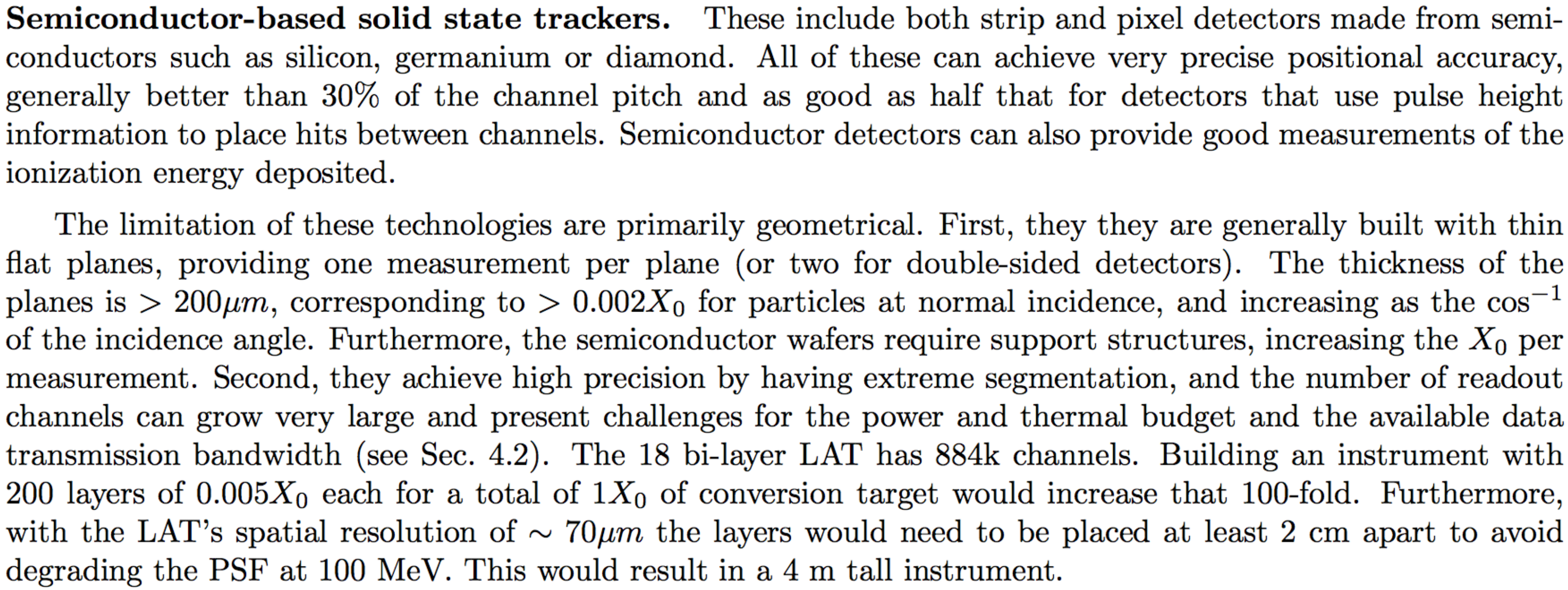

**Semiconductor-based solid state trackers.** These include both strip and pixel detectors made from semiconductors such as silicon, germanium or diamond. All of these can achieve very precise positional accuracy, generally better than 30% of the channel pitch and as good as half that for detectors that use pulse height information to place hits between channels. Semiconductor detectors can also provide good measurements of the ionization energy deposited.

The limitation of these technologies are primarily geometrical. First, they they are generally built with thin flat planes, providing one measurement per plane (or two for double-sided detectors). The thickness of the planes is $> 200\mu m$, corresponding to $> 0.002X_0$ for particles at normal incidence, and increasing as the $\cos^{-1}$ of the incidence angle. Furthermore, the semiconductor wafers require support structures, increasing the $X_0$ per measurement. Second, they achieve high precision by having extreme segmentation, and the number of readout channels can grow very large and present challenges for the power and thermal budget and the available data transmission bandwidth (see Sec. 4.2). The 18 bi-layer LAT has 884k channels. Building an instrument with 200 layers of $0.005X_0$ each for a total of $1X_0$ of conversion target would increase that 100-fold. Furthermore, with the LAT's spatial resolution of $\sim 70\mu m$ the layers would need to be placed at least 2 cm apart to avoid degrading the PSF at 100 MeV. This would result in a 4 m tall instrument.

# Implication for Instrument Performance

**Time Projection Chambers.** TPCs work by using a near uniform electric field to drift charge carries produced by ionization to the sides of the detector, where they are read out by sensor pads, which provide positional information in both direction transverse to the drift direction. Positional information in the longitudinal direction comes from measuring the drift time of the charge carriers.

Advances in solid-state sensor technology have made it possible to build very small individual channels on the amplification and sensor pads, allowing for excellent ($50\mu m$ or better) resolution in the transverse directions. However, the diffusion of the charge carriers limits the positional resolution in the longitudinal direction, particularly for large gas TPCs. With careful tuning of the drift gas longitudinal resolutions of $< 200\mu m$ for 1 m scale TPCs have been achieved.

TPCs can also quantify the ionization, which is useful for particle identification and quantifying the energy lost by charge particles in the TPC. The latter is particularly important for reconstructing Compton-scattering events.

One advantage of gas TPCs is that the density of the gas is low enough that several position measurement can contribute to the direction measurement, giving an excellent PSF. Furthermore, the density can be tuned to optimize the $X_0$ per-measurement. However, even the densest gases would require extreme pressures to provide enough target material for pair-conversion to reach LAT-like level; e.g., using Xe would require 50 bar of pressure at 300 K to reach $1X_0/\mathrm{m}$. This suggests either segmented TPC cells with converter material between them, or placing converter material in the TPC.

Gas TPCs have other potential disadvantages. 1) The lower resolution in the longitudinal direction. 2) The difficulties in keeping the gas tuned for optimal performance. 3) The degradation of the gas and the readout sensor from chemical interaction between the two. 4) The difficulties in operating high-pressure gas systems in orbit. These last two suggest that the drift gas is potentially a mission-limiting consumable. On the other hand, it is worth noting that gas-based detection systems have been used successfully in several mission.

Solid-state (i.e., drift-detectors) or liquid TPCs offer less flexibility in tuning the $X_0$ per-measurement, but are also somewhat less difficult to operate in orbit. However, it is worth nothing that liquid Ar (as in LArGO) requires substantial cooling, potentially creating a mission-limiting consumable or increasing the heat load on the spacecraft radiators.

# Implication for Instrument Performance

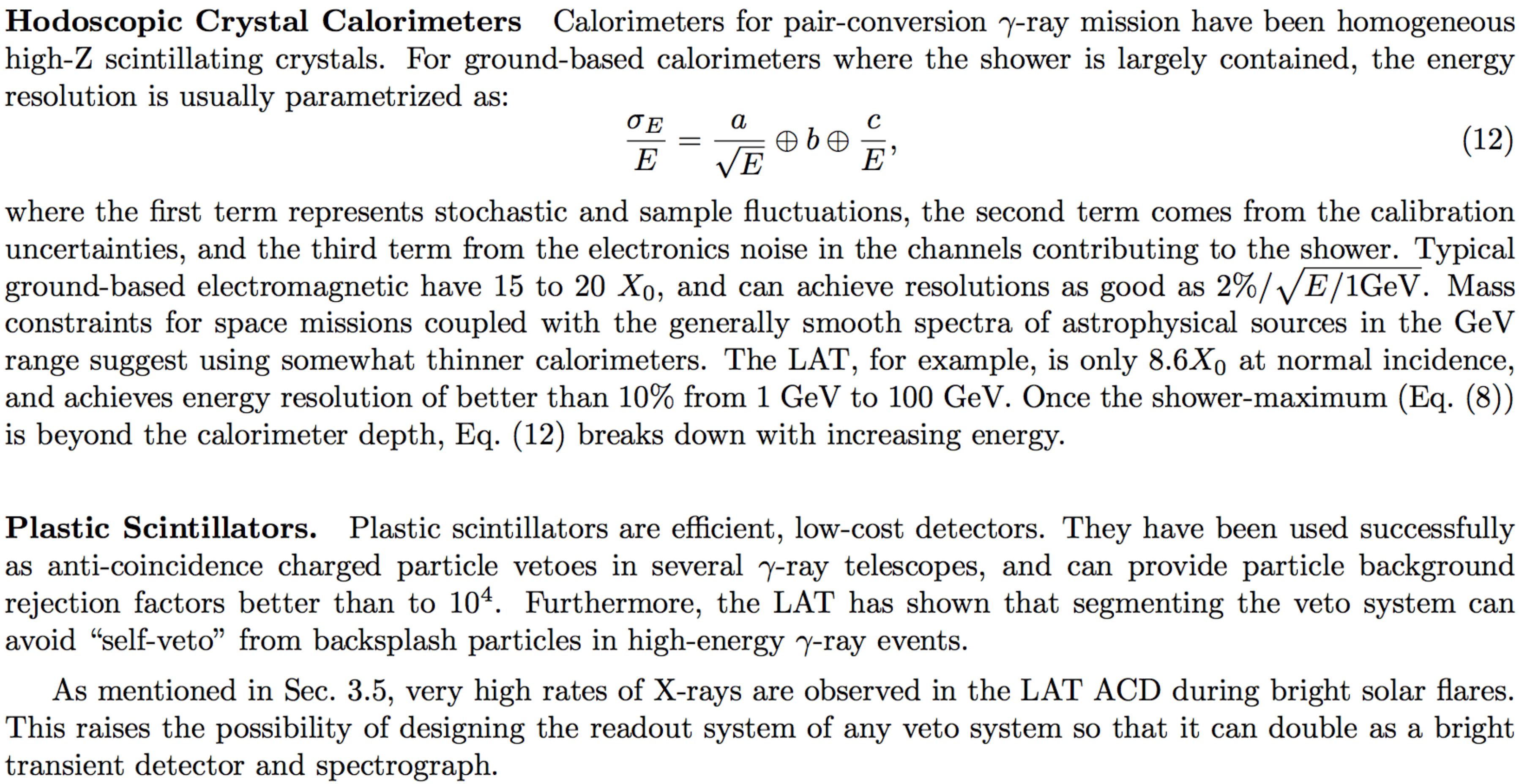

**Hodoscopic Crystal Calorimeters** Calorimeters for pair-conversion $\gamma$-ray mission have been homogeneous high-Z scintillating crystals. For ground-based calorimeters where the shower is largely contained, the energy resolution is usually parametrized as:

$$\frac{\sigma_E}{E} = \frac{a}{\sqrt{E}} \oplus b \oplus \frac{c}{E}, \qquad (12)$$

where the first term represents stochastic and sample fluctuations, the second term comes from the calibration uncertainties, and the third term from the electronics noise in the channels contributing to the shower. Typical ground-based electromagnetic have 15 to 20 $X_0$, and can achieve resolutions as good as $2\%/\sqrt{E/1\mathrm{GeV}}$. Mass constraints for space missions coupled with the generally smooth spectra of astrophysical sources in the GeV range suggest using somewhat thinner calorimeters. The LAT, for example, is only $8.6X_0$ at normal incidence, and achieves energy resolution of better than 10% from 1 GeV to 100 GeV. Once the shower-maximum (Eq. (8)) is beyond the calorimeter depth, Eq. (12) breaks down with increasing energy.

**Plastic Scintillators.** Plastic scintillators are efficient, low-cost detectors. They have been used successfully as anti-coincidence charged particle vetoes in several $\gamma$-ray telescopes, and can provide particle background rejection factors better than to $10^4$. Furthermore, the LAT has shown that segmenting the veto system can avoid "self-veto" from backsplash particles in high-energy $\gamma$-ray events.

As mentioned in Sec. 3.5, very high rates of X-rays are observed in the LAT ACD during bright solar flares. This raises the possibility of designing the readout system of any veto system so that it can double as a bright transient detector and spectrograph.

# Discussion

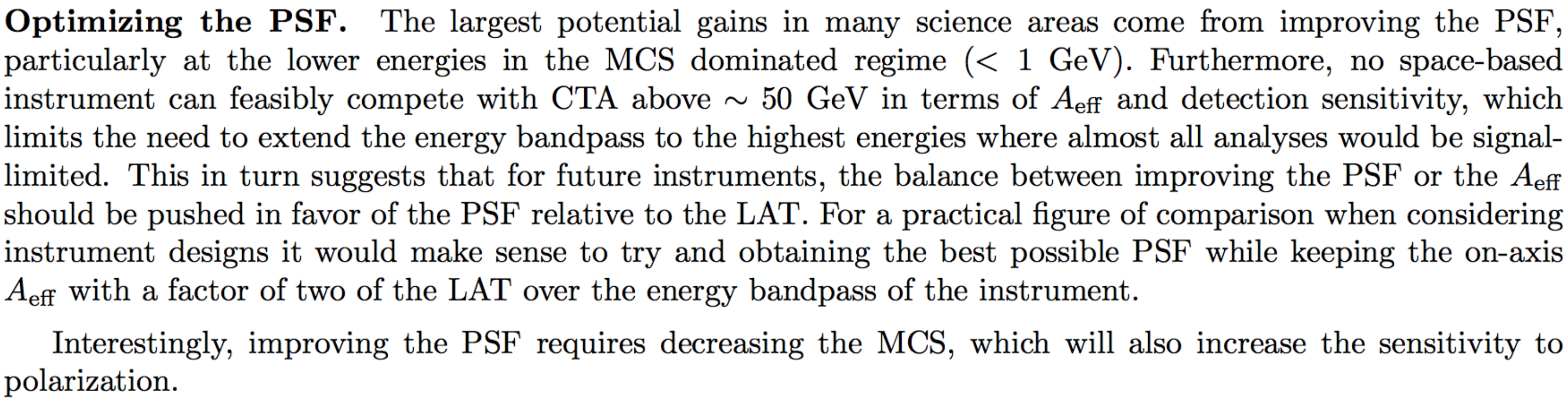

**Optimizing the PSF.** The largest potential gains in many science areas come from improving the PSF, particularly at the lower energies in the MCS dominated regime ($< 1$ GeV). Furthermore, no space-based instrument can feasibly compete with CTA above $\sim 50$ GeV in terms of $A_{\rm eff}$ and detection sensitivity, which limits the need to extend the energy bandpass to the highest energies where almost all analyses would be signal-limited. This in turn suggests that for future instruments, the balance between improving the PSF or the $A_{\rm eff}$ should be pushed in favor of the PSF relative to the LAT. For a practical figure of comparison when considering instrument designs it would make sense to try and obtaining the best possible PSF while keeping the on-axis $A_{\rm eff}$ with a factor of two of the LAT over the energy bandpass of the instrument.

Interestingly, improving the PSF requires decreasing the MCS, which will also increase the sensitivity to polarization.

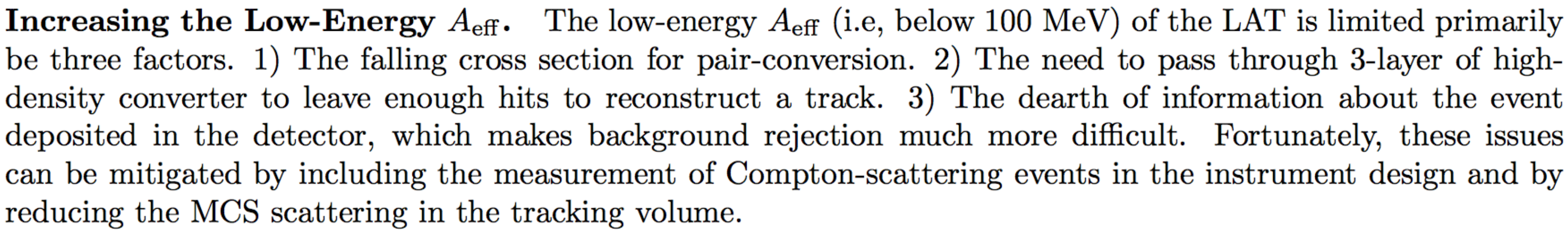

**Increasing the Low-Energy $A_{\rm eff}$.** The low-energy $A_{\rm eff}$ (i.e, below 100 MeV) of the LAT is limited primarily be three factors. 1) The falling cross section for pair-conversion. 2) The need to pass through 3-layer of high-density converter to leave enough hits to reconstruct a track. 3) The dearth of information about the event deposited in the detector, which makes background rejection much more difficult. Fortunately, these issues can be mitigated by including the measurement of Compton-scattering events in the instrument design and by reducing the MCS scattering in the tracking volume.

# Discussion

**Choosing the FOV and the Instrument Geometry.** The large FOV of the LAT and the all-sky survey mode it allowed has enabled many breakthroughs and is well-suited to the highly variable nature of many $\gamma$-ray emitting sources. It is worth recalling that the FOV of the LAT is 2.5 sr as compared to the un-occulted sky in low Earth orbit of 8.4 sr or 12.6 sr for the whole sky. Thus, the maximum potential gain in the FOV is somewhere between a factor of 3.5 to 5, depending on the orbit. Although not huge, this could be combined with a factor of 2 to 3 increase in the average effective area to obtain a factor of 10 increase in the acceptance without hugely increasing the size of the instrument, an important limitation in space missions.

On the other hand, the best ways to improve the PSF are to decreases the density of the material in the tracker and to space the tracking element further apart. Given the space limitations, both of these could result in a FOV that is somewhat smaller than the LAT's. These considerations present two alternate instrument geometries as opposite extremes to consider.

The first, designed to have an excellent PSF and a limited FOV, would be tall and relatively narrow, and maximize the lever-arm in the direction of travel of the incoming $\gamma$ rays. Such an instrument would be suited to an observing strategy of scanning the Galactic plane with occasional pointings and limited surveys of high-Galactic latitude sources and regions.

The second, designed to maximize the FOV while retaining a very good PSF, would be as compact as possible for a given surface area, i.e., cubic or spherical. In this geometry, one of the challenges it so avoid building an intrinsic directionality into the instrument, e.g., a design with a tracker above a calorimeter is only sensitive to $\gamma$ rays going "down", can not exceed a FOV 6.3 sr, and is unlikely to do better than about FOV 3 sr unless the tracker is extremely squat. So, in this case it is worth considering novel geometries, such a calorimeter sandwiched between two trackers.

An interesting alternative is the possibility of a "monolithic" instrument, i.e., one with a single sub-system that measures both the direction and energy of the incoming $\gamma$ rays. In practice, this likely would be done in one of three ways, each of which would present substantial design challenges. 1) Adding a magnet to measure the momenta of the charged particles in the tracking volume. 2) Building a particle tracker that is several radiation lengths thick. 3) Increasing the readout granularity of a hodoscopic calorimeter to extent that it does not limit the PSF.

# Conclusion

**Summary** We have presented a series of summaries of information that may be useful in the design of future high-energy $\gamma$-ray telescopes. Specifically, we have summarized the instrument performance factors critical for scientific goals, the physical mechanisms influencing the detector design, and the most popular detector technologies. We have also laid out the key trade-offs that must be considered.

Almost all of this information is available in greater detail elsewhere. However, we hope that this contribution will prove useful by consolidating the material in a single source.